The Isopeptidase USP2a Protects Human Prostate Cancer from Apoptosis

Carmen Priolo,[1,5,7] Dan Tang,[1] Mohan Brahamandan,[1] Barbara Benassi,[1,5] Ewa Sicinska,[1] Shuji Ogino,[1,2] Antonella Farsetti,[5,6] Alessandro Porrello,[4,5] Stephen Finn,[1] Johann Zimmermann,[3] Phillip Febbo,[4] and Massimo Loda[1,2]

[1]Medical Oncology, Dana-Farber Cancer Institute and [2]Pathology Department, Brigham and Women's Hospital, Harvard Medical School, Boston, Massachusetts; [3]Novartis Pharma, Oncology Research, Basel, Switzerland; [4]Institute for Genome Sciences and Policy, Duke University, Durham, North Carolina; and [5]Departments of Medical Oncology and Experimental Oncology, Regina Elena Cancer Institute, [6]INeMM, National Research Council and [7]Endocrinology, Catholic University, Rome, Italy

Abstract

Deubiquitinating enzymes can prevent the destruction of protein substrates prior to proteasomal degradation. The ubiquitin-specific protease 2a (USP2a) deubiquitinates the antiapoptotic proteins Fatty Acid Synthase and Mdm2. Here, we show that when USP2a is overexpressed in nontransformed cells, it exhibits oncogenic behavior both *in vitro* and *in vivo* and prevents apoptosis induced by chemotherapeutic agents. Notably, USP2a silencing in several human cancer cell lines results in apoptosis. Gene set enrichment analysis, which focuses on groups of genes sharing biological function or regulatory pathways, was done on microarray expression data from human prostate cancers. The cell death–related gene set, as well as a selected cluster of validated p53 target genes, were significantly enriched in the low USP2a expression group of tumors. Conversely, genes implicated in fatty acid metabolism were significantly associated with tumors expressing high USP2a (44%). The expression profile analysis is consistent with the effects of USP2a on its known targets, i.e., Fatty Acid Synthase and Mdm2, defining a subset of prostate tumors resistant to apoptosis. USP2a thus represents a therapeutic target in prostate cancer. (Cancer Res 2006; 66(17): 8625-32)

Introduction

Selective degradation of proteins through ubiquitination involves the activation of a signaling cascade that results in the covalent attachment of a poly-ubiquitin chain to protein targets (1). This modification occurs through the formation of isopeptide bonds between ubiquitin and the target protein. The formation of a poly-ubiquitin chain acts as a signal for degradation by the proteasome (2). Ubiquitination of targeted substrates, however, is a reversible process. The ubiquitin-specific proteases (USP) are cysteine proteases, part of a more general class of proteolytic enzymes known as deubiquitinating enzymes (1, 3). Despite the large number of USPs identified, relatively little is known about their physiologic roles or their substrates. USPs may "edit" the number of ubiquitin moieties in the poly-ubiquitin chain of poorly or erroneously ubiquitinated proteins or generate free ubiquitin from poly-ubiquitin chains released after proteasomal activity. The large number of USP family members and their limited homology outside of the active catalytic sites also suggest a specificity of interaction with defined substrates. Importantly, a pre-proteasomal action for isopeptidases has been shown. This results in the cleavage of the poly-ubiquitin tag from specific substrates, preventing and modulating their degradation. Specifically, the deubiquitinating enzyme HAUSP (USP7) is a key regulator of both p53 and Mdm2 (4–6). In addition, the familial cylindromatosis tumor suppressor gene (*CYLD*) modulates the activity of nuclear factor κB via a similar mechanism (7, 8). Finally, we showed that USP2a associates with and prolongs the half-life of Fatty Acid Synthase (FAS; ref. 9). FAS, itself an androgen-regulated gene, is overexpressed in biologically aggressive prostate cancer, whereas its expression is negligible to absent in normal prostatic epithelium (reviewed in ref. 10). Importantly, RNA interference of USP2a results in apoptosis which, in the androgen-dependent LNCaP cells, is rescued by FAS overexpression (9).

Prostate cancer is the most frequently diagnosed, non–dermatologic cancer in men (11). Androgen ablation therapy remains the only treatment that prolongs life for men with metastatic prostate cancer. Although docetaxel-based therapy has recently been shown to affect tumor growth and improve cancer-related symptoms and quality-of-life end points, there is still a pressing need for therapy that might affect outcome (12, 13). Thus, novel therapeutic targets need to be identified.

Here, we show that USP2a displays canonical oncogenic properties such as colony formation, growth in soft agar, and tumor formation in nude mice when introduced in nontransformed immortalized prostate epithelial cells or immortalized murine fibroblasts. We also show that USP2a overexpression in immortalized prostate epithelial cells confers resistance to apoptosis induced by chemotherapeutic agents, whereas USP2a RNA interference results in apoptosis in a variety of tumor cell lines. Stevenson et al. now show that Mdm2 is also a target of USP2a, thus, potentially affecting p53-mediated apoptosis.[8] Gene profiling of human prostate tumors overexpressing USP2a (44% of cases) revealed an association with increased expression of genes involved in fatty acid metabolic pathways, whereas targets of p53-mediated suppression were similarly up-regulated. In contrast, cell death–associated and p53-target genes were up-regulated in tumors with low USP2a expression. Such events can contribute to enhancing resistance to apoptosis in prostate cancer cells that

Note: Supplementary data for this article are available at Cancer Research Online (http://cancerres.aacrjournals.org/).

Requests for reprints: Massimo Loda, Dana-Farber Cancer Institute, D1536, 44 Binney Street, Boston, MA 02115. Phone: 617-632-4001; Fax: 617-632-4005; E-mail: massimo_loda@dfci.harvard.edu.

©2006 American Association for Cancer Research.

doi:10.1158/0008-5472.CAN-06-1374

[8] L.F. Stevenson, A. Sparks, D.P. Xirodimas, D.P. Lane, M.K. Saville. The deubiquitinating enzyme USP2a regulates the p53 pathway by targeting Mdm2. Personal communication, 2006.

Downloaded from cancerres.aacrjournals.org on May 28, 2017. © 2006 American Association for Cancer Research.

overexpress this isopeptidase. These results, together with the resolution of the crystal structures of both USP2[9] and FAS (14), provide the rationale for USP2a targeting in prostate cancer.

Materials and Methods

Generation of wild-type and mutant USP2a–overexpressing cell lines. Immortalized androgen receptor (AR)-expressing prostate epithelial cells (AR-iPrEC; ref. 15; a gift from W.C. Hahn, Dana-Farber Cancer Institute, Boston, MA) were infected with pBABE retroviral constructs of wild-type (AR-iPrEC-USP2a-wt) and catalytic mutant (C276A and H549R; AR-iPrEC-USP2a-mut) HA-tagged *USP2a* genes, containing a puromycin resistance gene. Infection of pBABE vector alone (AR-iPrEC-EV) was used as a control. Cells were transduced through infection using polybrene (10 μg/mL) and selected in the presence of 1.6 μg/mL puromycin. pHE482 retroviral constructs of wild-type and catalytic mutant (C276A) *USP2a* were used to infect immortalized murine fibroblast (NIH3T3).

Colony formation assay. AR-iPrEC-USP2a-wt (wt), AR-iPrEC-USP2a-mut (mut), and AR-iPrEC-EV (EV) cells were seeded in triplicate in 100 mm plates (1,000 cells/plate) in PrEBM medium (Cambrex, East Rutherford, NJ). After 14 days, cells were fixed and stained with 0.5% crystal violet before counting.

Soft agar assay. One thousand AR-iPrEC cells (infected with wt, mut, and EV constructs) were resuspended with 0.4% agarose (Difco agar Noble from Becton Dickinson, Sparks, MD) in PrEBM and seeded in triplicate in six-well plates coated with 0.8% agar. Colonies with >30 cells were counted after 2 weeks by staining with 0.4 mg/mL of Neutral Red.

Cell transfections with anti-USP2a small interfering RNA. LNCaP, DU145, and PC-3 cells as well as the following non–prostate carcinoma lines: SW480, LOVO, SW620, HCT15 (colon cancer), BT549, SKBR3 (breast cancer), HT1080, MG63, and MNN4/HOS (sarcoma) were used for small interfering RNA (siRNA) experiments. Cells (2.5×10^5) were seeded in 60 mm plates in the specific medium (RPMI without phenol red supplemented with 10% fetal bovine serum and penicillin/streptomycin for LNCaP and MEM-α supplemented with 10% fetal bovine serum and gentamicin for the other cells) and 24 hours later, transfected with 80 nmol/L anti-USP2a siRNA [r(UGCUUGUGCCCGGUUCGAC)d(TT)] or 80 nmol/L siControl non-targeting siRNA no. 2 (Dharmacon, Lafayette, CO) as previously described (9). Forty-eight, 72, and 120 hours posttransfection, cells were collected for assessing USP2a knockdown and apoptosis.

Treatments with chemotherapeutic agents. AR-iPrEC-USP2a-wt (wt), AR-iPrEC-USP2a-mut (mut), and AR-iPrEC-EV (EV) cells were seeded in 60 mm Petri dishes (5×10^5 cells/dish) in PrEBM and treated 24 hours after plating with 2 or 7.5 μg/mL of cisplatin (Calbiochem, La Jolla, CA) and 25 or 100 nmol/L of paclitaxel (Calbiochem) for 24, 48 and 72 hours. At the end of each drug administration, cells were harvested to evaluate apoptosis.

Apoptosis and proliferation assays. Following anti-USP2a siRNA transfection and drug treatments, cells were collected and fixed overnight at 4°C with 75% ethanol for propidium iodide staining and flow cytometry (fluorescence-activated cell sorting, FACS) analysis. Protein extracts were assayed for cleaved-PARP expression by Western blot. Proliferation rate was assessed in AR-iPrEC cells overexpressing mut and wt USP2a by 5-bromo-2-deoxyuridine (BrdUrd) staining (4 hours) and subsequent FACS analysis.

Western blot. Equal amounts of total proteins were separated on 4% to 12% Tris-glycine SDS-PAGE gels (Invitrogen, Carlsbad, CA) and transferred for 4 hours to polyvinylidene difluoride membrane. The membrane was blocked in 5% milk-PBS-0.05% Tween 20 for 1 hour and then incubated overnight with the primary antibody.

The following antibodies were used: L523 and N-term anti-USP2a (Abgent, San Diego, CA) at 1:400 dilution, HA.11 anti-HA (Covange, Berkeley, CA) at 1:1,000 dilution, Asp214 anti-cleaved PARP (Cell Signaling, Danvers, MA) at 1:1,000 dilution, mouse anti-FAS (BD Transduction Laboratories) at 1:2,000 dilution, DO-1 anti-p53 (Santa Cruz Biotechnology, Santa Cruz, CA) at 1:500 dilution, Ab-1 anti-Mdm2 (Calbiochem) at 1:100 dilution, C-19 anti-p21 (Santa Cruz Biotechnology) at 1:400 dilution and anti-β-actin (Sigma, St. Louis, MO) at 1:10,000 dilution.

Generation of xenografts. NIH3T3 cells overexpressing wild-type and catalytic mutant USP2a (NIH3T3-USP2a-wt, NIH3T3-USP2a-mut, and NIH3T3-EV) were assayed for *in vivo* tumorigenicity in 6- to 8-week-old male nude mice (*nu/nu*, from Charles River Laboratories, Wilmington, MA). NIH3T3-USP2a-wt cells (3×10^5) mixed with Matrigel (BD Biosciences, Bedford, MA) were injected s.c. in the right flank of 12 mice, whereas NIH3T3-USP2a-mut (C276A) and control cells (NIH3T3-EV) were injected in the left flank of the same mouse. Animals were monitored twice weekly and sacrificed after 3 weeks by CO_2 inhalation. Mice were injected i.p. with BrdUrd (Roche, Indianapolis, IN) 5 hours prior to sacrifice. S.c. tumors were fixed in 10% neutral buffered formalin and paraffin-embedded for histopathologic exam and BrdUrd staining. Tumor volume (V) was calculated by the formula $V = abb / 2$, where a represents the minimum and b the maximum tumor diameter (16).

Human prostate tissue samples. From 1995 to 1997, samples of prostate tumors and adjacent prostate tissue not containing tumor (referred to as "normal") were collected from patients undergoing radical prostatectomy at the Brigham and Women's Hospital as previously described (17). Quantitative PCR (qPCR) for USP2a was done in 32 tumors in which RNA was still available.

Paraffin blocks corresponding to the samples used for mRNA expression analysis were retrieved, the appropriate areas of cancer were marked, and tissue microarrays were generated with triplicate normal and tumor cylinders for each patient. Five-micron sections from these arrays were used in immunohistochemistry experiments.

Real-time reverse transcription-PCR and sequencing. One microgram of RNA from human prostate tissues and cells overexpressing wt and mut USP2a (AR-iPrEC and NIH3T3) or transfected with anti-USP2a siRNA was reverse-transcribed with SuperScript III Platinum two-step qRT-PCR kit (Invitrogen). qPCR was done with the ABI Prism 7300 PCR instrument (Applied Biosystems, Foster City, CA) by using the SYBR green master mix (Applied Biosystems). The mRNA amount of each gene was calculated using the standard curve method (4 log. dilutions in triplicate) and data were analyzed with SDS 2.2 software (Applied Biosystems). The following primers were used to measure *USP2a* mRNA levels: forward 5′-TGCTGAGACCCGACATCACT-3′; reverse 5′-TGGGGTCTATCCGGTAGCTA-3′. The relative abundance of *USP2a* transcript was normalized to *GAPDH* levels (human *GAPDH*: forward primer 5′-GCCTGTGAGTGAGTGCAGAA-3′, reverse primer 5′-ATCTCTGTCGTCGTCCTCGT-3′; mouse *GAPDH*: forward primer 5′-AACTTTGGCATTGTGGAAGG-3′, reverse primer 5′-TGTGAGGGAGATGCTCAGTG-3′) using the $2^{-\Delta\Delta Ct}$ method (18).

Twenty human prostate tumors were analyzed for USP2a mutations by cDNA sequencing. Four regions spanning the entire mRNA of USP2a were amplified (RT-PCR) and sequenced by using the following primers: (*a*) forward primer 5′-ATGTCCCAGCTCTCCTCCAC-3′, reverse primer 5′-AGCCCCTGCAGGGTGCAG-3′; (*b*) forward primer 5′-AGTGACCAACAACTGCCTCAG-3′, reverse primer 5′-TGTGTGTGCATTGCTGCCGTG-3′; (*c*) forward primer 5′-ATTACTGCCTCCAGAGGCTCTAC-3′, reverse primer 5′-TCAGACGGAGCACCAAGATCTTTG-3′; (*d*) forward primer 5′-ATGTGCTTGATGGAGATGAAAAG-3′, reverse primer 5′-CTACATTCGGGAGGGCGG-3′. The cycling conditions used for these PCRs were as follows: 95°C for 2 minutes, 30 cycles of 95°C for 30 seconds, 51°C for 30 seconds, and 72°C for 45 seconds, with a final extension step of 72°C for 5 minutes.

Gene expression profiling and gene set enrichment analysis. Previously published U95Av2 microarray data for 52 prostate tumors were processed with MAS4 (Affymetrix, Santa Clara, CA) and scaled together as previously described (17).[10] Of the 52 tumors, 32 also had qPCR data for *USP2a* and *GAPDH*. These 32 samples were ranked according to *USP2a* expression by qPCR (ΔCT, USP2a versus GAPDH). The 32 samples were split

[9] M. Renatus, S.G. Parrado, M. Kroemer, A. D'Arcy, D. Vinzenz, U. Eidhoff, R. Riedl, U. Hassiepen, S. Worpenberg, B. Pierat, B. Gerhartz. Structural basis of ubiquitin recognition by the deubiquitinating protease USP-2. Structure 2006;14, in press.

[10] Available as "Prostate_T_allmeansquare.res" at http://www.broad.mit.edu/cgi-bin/cancer/datasets.cgi.

Downloaded from cancerres.aacrjournals.org on May 28, 2017. © 2006 American Association for Cancer Research.

into tertiles; gene set enrichment analysis (GSEA v1.0; ref. 19)[11] was applied to identify gene sets differentially expressed between the subset of samples with high expression of *USP2a* (n = 11) and samples with low *USP2a* expression (n = 11; file "Prostate_T_allmeansquare_USP2_DeltaCT.res", available on request). GSEA variables used included: ranking statistic, signal to noise (S2N); scoring scheme, weighted; permute, phenotype; permutation number, 1,000; gene set size restrictions, 10 minimum, 500 maximum; and gene set collection, "s2.hgu95av2.xls" (available as Supplemental Table S1). Samples in the middle tertile (n = 10) or without qPCR data for *USP2a* (n = 20) were excluded from the analysis. Four hundred and forty gene sets and biological pathways were examined in this GSEA, and gene sets with normalized enrichment scores below a false discovery rate of 0.25 were considered significant. An independent GSEA was done on a customized gene set of 24 p53 target genes (available as Supplemental Table S2) whose accession numbers are recorded in a .gmt file (available on request). In this last analysis, multiple entries associated with each gene were allowed, in order to take into account all the available genomic information contained in the examined U95Av2 GeneChips.

Immunohistochemistry. Immunostaining was done on formalin-fixed paraffin-embedded samples (TMA blocks) and s.c. murine xenografts as previously described (20). The following primary antibodies were used: N-term anti-USP2a (Abgent) at 1:50 dilution, IF-2 anti-Mdm2 (Calbiochem) at 1:100 dilution, rabbit anti-FAS (Assay Designs, Ann Arbor, MI) at 1:100 dilution, and anti-BrdUrd (BD) at 1:100 dilution.

Results

USP2a is overexpressed in human prostate adenocarcinomas. We have previously shown that the deubiquitinating enzyme USP2a is androgen-regulated and that it interacts with FAS. In addition, using androgen-dependent prostate cancer cells, we showed that USP2a inactivation results in apoptosis, which can be rescued by FAS overexpression (9).

In order to address the relevance of these findings in human prostate cancer, we first used a qPCR strategy to determine the degree to which *USP2a* was overexpressed in resected prostatic adenocarcinomas. Five putative isoforms of *USP2* have been described (21). Primers specific for the *USP2a* isoform were used in the qPCR experiment. RNA was extracted from tumor-enriched (macrodissected) human prostatectomy samples (17). Adjacent normal tissue served as control. Thirteen of 32 tumors (44%) showed 1.6- to 104-fold (median, 5.47-fold) *USP2a* expression relative to normal tissues (Fig. 1*A*). In addition, we confirmed the presence of the protein by immunohistochemistry only in some, optimally fixed, corresponding paraffin-embedded samples. Cytoplasmic positive immunostaining was mostly detected in tumor glands, whereas in normal prostatic epithelium, USP2a expression was restricted to the basal cells (Fig. 1*B*). Twenty prostate tumors were also analyzed for USP2a mutations by cDNA sequencing. No mutations were found in these samples.

USP2a overexpression transforms human immortalized prostate epithelial cells *in vitro*. Having established that USP2a is overexpressed in a significant number of human adenocarcinomas, we next decided to determine whether ectopic expression of USP2a conferred a selective growth advantage to nontransformed prostate epithelial cells (PrEC) *in vitro*. PrEC cells were first immortalized with SV40 early region and hTERT and induced to display a "secretory" phenotype to mimic human prostate cancer by stable infection of the androgen receptor. Subsequent transformation is achieved in these cells only by the addition of

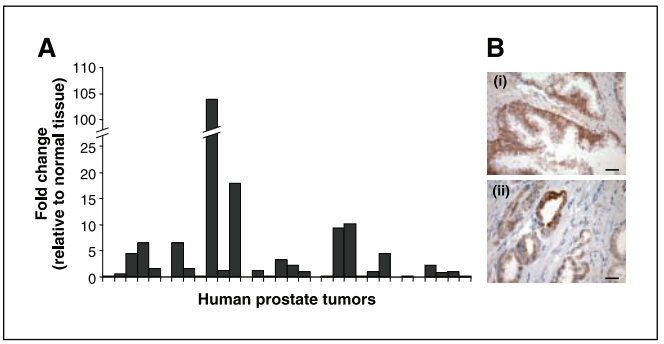

Figure 1. USP2a expression in human prostate tumors. *A,* USP2a mRNA expression was analyzed in a cohort of 32 human prostate tumors by qRT-PCR and normalized to relative normal tissue. Thirteen of 32 tumors (44%) showed 1.6- to 104-fold (median, 5.47-fold) USP2a expression relative to normal tissues. *B,* immunohistochemistry for USP2a in a formalin-fixed, paraffin-embedded human prostate sample (from *A*). Cytoplasmic positive immunostaining was detected in tumor glands (*ii*), whereas in normal prostatic epithelium, USP2a expression was restricted to the basal layer (*i*); *bars,* 100 μm.

potent oncogenes such as ^{12}Vras (15). We infected AR-iPrEC cells using retroviral constructs of wild-type and catalytic double mutant (C276A and H549R) HA-tagged *USP2a* (Fig. 2*A*). Clonogenic assays were done on AR-iPrEC cells overexpressing wild-type (AR-iPrEC-USP2a-wt) and mutant (AR-iPrEC-USP2a-mut) HA-tagged USP2a and on the same cells infected with the retroviral vector alone (EV). The number of colonies was significantly increased in cells overexpressing wild-type USP2a compared with the control (Fig. 2*B*) and was intermediate between the latter and ^{12}Vras-infected cells (data not shown).

When grown in soft agar, wild-type USP2a cells also had significantly increased number and size of colonies compared with both parental cells and to those transfected with mutant USP2a (Fig. 2*C*).

To assess whether these wild-type USP2a cells acquired their growth advantage through an induction of proliferative potential, BrdUrd incorporation assays were also done. No significant difference in proliferative rate was found between cells overexpressing wild-type or mutant USP2a compared with control (data not shown).

USP2a has *in vivo* tumorigenic properties. We next tested whether overexpression of USP2a resulted in a growth advantage *in vivo*. To do this, we engineered NIH3T3 cells to stably overexpress both the wild-type and the catalytic mutant (C276A) USP2a (Fig. 3*A*). Engineered NIH3T3 cells were injected s.c. with Matrigel (3×10^5/mouse flank) in 12 nude mice. Importantly, cells expressing wild-type USP2a, but not those infected with its catalytically inactive mutant, were able to transform NIH3T3 cells. S.c. tumors (0.2-0.9 cm^3) grew within 3 weeks in 12 of 12 nude mice injected with cells overexpressing wild-type USP2a, whereas no tumors developed in hosts injected with either mock- or mutant USP2a-infected cells (Fig. 3*B* and *C*). Histopathologically, all s.c. neoplasms showed a sarcomatous phenotype as expected after transformation of fibroblasts (Fig. 3*D*). The proliferation rate in these tumors was considerably higher than in controls as assessed by both mitotic rate (22 ± 8 mitoses per high power field), and BrdUrd incorporation (35 ± 5% of positive nuclei per high power field). Neither BrdUrd-positive staining nor mitotic figures were found in controls at appreciable levels. Taken together, these results suggest that USP2a overexpression transforms NIH3T3 cells *in vivo*.

[11] http://www.broad.mit.edu

Downloaded from cancerres.aacrjournals.org on May 28, 2017. © 2006 American Association for Cancer Research.

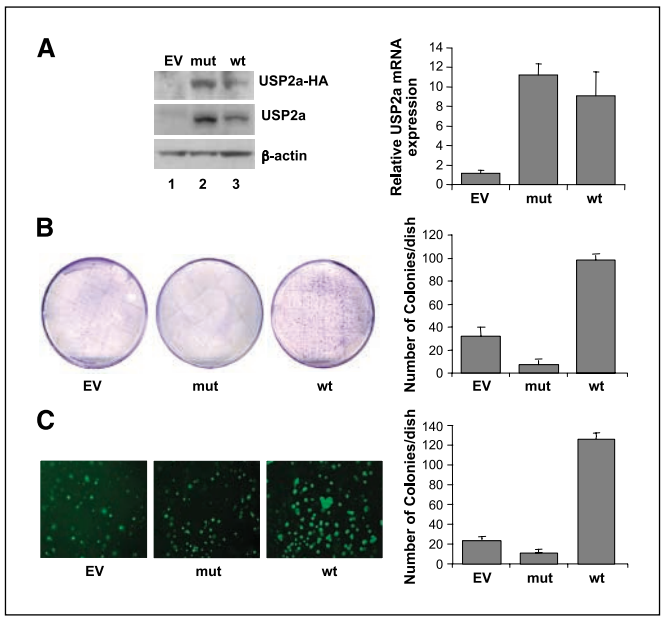

Figure 2. Oncogenic properties of wild-type but not mutant USP2a in nontransformed, immortalized prostate epithelial cells. *A,* expression of catalytic mutant (*mut, lane 2*) and wild-type (*wt, lane 3*) HA-tagged USP2a in AR-iPrEC cells by Western blot (*left*) and qPCR (*right*). *Lane 1* (*EV*), control. Colony formation (*B*) and growth in soft agar assays (*C*) on the same cells. *Columns,* mean of three experiments done in triplicate; *bars,* ±SD (*right*).

GSEA reveals that expression of distinct gene families is associated with USP2a abundance in prostate adenocarcinomas. Having established oncogenic properties of USP2a *in vitro* and *in vivo* and determined the prevalence of USP2a overexpression in human samples, we next wanted to investigate whether prostate adenocarcinomas overexpressing USP2a were associated with specific gene expression profiles. To this end, we used microarray data we had previously generated from prostate adenocarcinomas (17). These included the 32 cases characterized here for *USP2a* expression by qRT-PCR. Because Affymetrix chips are constructed in such a way that 3′-end oligonucleotides are preferentially used to detect and quantify gene expression, distinction between the various isoforms of *USP2* (21) was not achievable. To select exclusively USP2a-overexpressing tumors, the relative *USP2a* mRNA expression among tumors obtained by qRT-PCR was used to classify 32 tumors in tertiles, i.e., high, intermediate, and low *USP2a* levels. In these three groups, the *GAPDH*-normalized (ΔCt) values (18) were ≤5.4, >5.4 and <8, and ≥8, respectively. In order to assess whether USP2a-related gene expression patterns could define the biological differences between prostate tumors, a GSEA (19) was done on microarray expression data (U95Av2) from these 32 human prostate cancers (Fig. 4*A*). GSEA derives its power by focusing on the analysis of groups of genes that share biological function, chromosomal location, or regulatory pathways. Remarkably, when the top one-third of tumors (n = 11) were compared with the bottom one-third (n = 11), the only gene set (out of 440 tested) significantly enriched in the low *USP2a* expression group was the gene set of cell death–related genes. In addition, because of the established relationship between USP2a, Mdm2, and p53 we selected a set of 24 validated p53 target genes mostly involved in proapoptotic pathways to be tested in GSE analysis. Of note, this customized gene set was also significantly associated (false discovery rate, 0.022) with tumors expressing low levels of *USP2a* (Supplemental Table S2). Our finding is in keeping with the newly discovered Mdm2 stabilizing function of this isopeptidase.[8]

The significant gene sets emerging from the analysis of tumors expressing high *USP2a* levels belong to pathways involved in fatty acid synthesis/metabolism, receptor tyrosine kinases (RTK), such as *ErbB3*, early endosome antigen 1 (*eea1*), and *rab*, as well as *STAT3* signaling (Fig. 4*A*). Thus, by focusing on gene sets sharing biological function, GSEA applied to this data set was able to reveal important pathways strongly associated with USP2a expression. In fact, in a single analysis, we confirmed the role played by USP2a in stabilizing FAS (9) and Mdm2[8] whereas the importance of ErbB3, as a partner of ErbB2 and of STAT3, has also been previously assessed in prostate cancer (22–24). Now these events have been tied to USP2a overexpression. Figure 4*B* displays an example of a USP2a-overexpressing tumor showing high expression in prostate cancer cells of the two proteins stabilized by USP2a, i.e., FAS (*i*) and Mdm2 (*ii*).

USP2a silencing results in apoptosis in cancer cells. *In vitro* transformation of AR-iPrEC cells by USP2a overexpression could not be attributed to the induction of proliferation. In addition, expression profiling of human prostate tumors showed that high USP2a expression levels were associated with the expression of antiapoptotic genes whereas cell death pathways were associated with low USP2a levels. In spite of the pro-proliferative action of USP2a in sarcomatous transformation, these data indicate a role for USP2a in protecting epithelial tumor cells from apoptosis, perhaps via its effect on either FAS or Mdm2, or both. We therefore transfected USP2a siRNA into malignant prostate epithelial cell lines (LNCaP, DU145, and PC-3) to assess whether this would have an effect on apoptosis. RNA and protein knockdown was assessed by quantitative RT-PCR and Western blot (Fig. 5*A*). Apoptosis was analyzed at 48, 72, and 120 hours after transfection by FACS analysis (propidium iodide) and Western blot (PARP cleavage). USP2a knockdown induced substantial and increasing levels of apoptosis in LNCaP (androgen dependent, wild-type p53) and DU145 (androgen independent, mutant p53) over time, but no significant induction of cell death was seen in PC-3 cells (androgen independent, p53 null). Taken together, these data suggest that USP2a provides resistance to apoptosis to prostate cancer cells. We next assessed whether USP2a knockdown affected both FAS and Mdm2 in LNCaP cells. Both of these proteins were substantially decreased by 48 hours (Fig. 5*C*), whereas p53 and its target, p21, increased. This suggests that in LNCaP cells, apoptosis induced by USP2a interference may be mediated by FAS or Mdm2 knockdown (with subsequent induction of p53 and its targets), or both.

To investigate whether USP2a displays antiapoptotic properties in other non–prostate human tumors, we silenced USP2a mRNA in nine additional cell lines (SW480, SW620, LoVO, HCT15, BT549, SKBR3, HT1080, MG63, and MNN4/HOS) derived from different human cancers (colon, breast, and sarcomas). USP2a knockdown induced a variable but appreciable apoptotic response in all cells tested (data not shown). Interestingly, the most significant induction of programmed cell death generally occurred in the lines with the highest levels of USP2a. These results suggest that USP2a knockdown induces an apoptotic response in diverse human tumors.

USP2a overexpression confers resistance to chemotherapeutic agents. Classifying prostate adenocarcinomas on the

Downloaded from cancerres.aacrjournals.org on May 28, 2017. © 2006 American Association for Cancer Research.

basis of USP2a overexpression provided biological data suggesting that USP2a is protective against programmed cell death. *In vitro* knock-down and overexpression experiments largely confirmed these findings. We therefore reasoned that USP2a overexpressing prostate cancer might be resistant to apoptosis induced by chemotherapeutic agents. In order to test this hypothesis, we set out to determine whether ectopic expression of USP2a confers resistance to apoptosis induced by selected chemotherapeutic agents in immortalized prostate epithelial cells. AR-iPrEC cells, with and without wild-type and mutant USP2a were treated with cisplatin and paclitaxel in a dose-dependent manner at the indicated time points (Fig. 6*A* and *B*). As expected, wild-type USP2a, but not the catalytically inactive mutant, conferred resistance to apoptosis induced by both cisplatin and paclitaxel (Fig. 6*A* and *B*). These data show that USP2a overexpression confers oncogenic properties to prostate epithelial cells *in vitro* preferentially by protecting them from apoptosis.

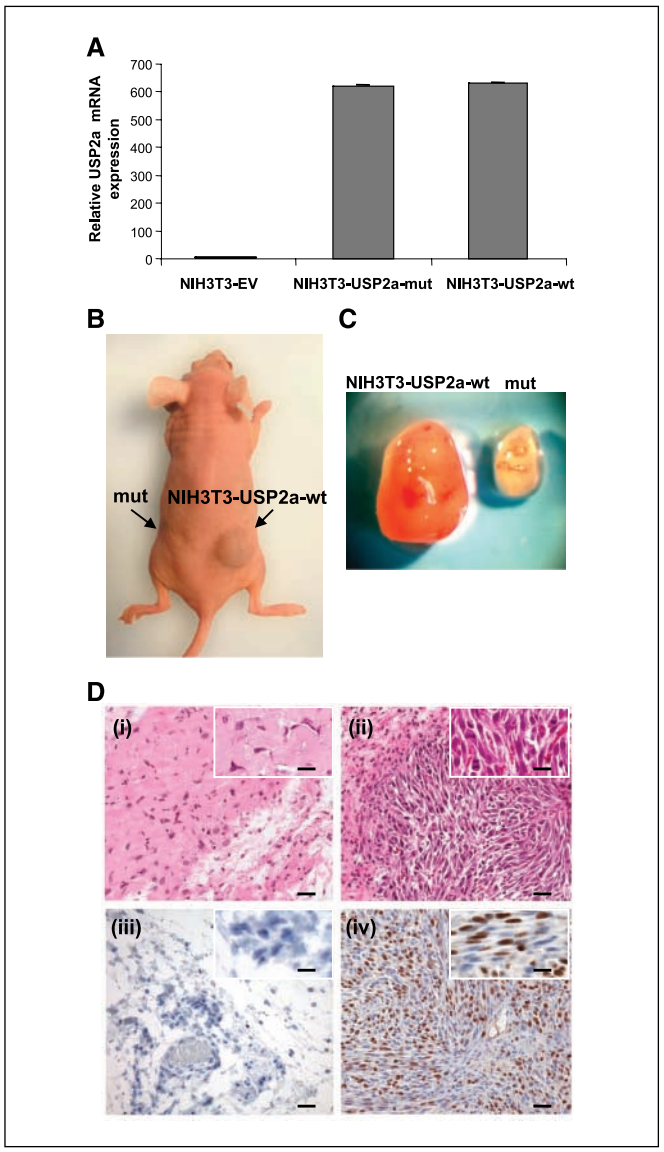

Figure 3. Generation of s.c. xenografts in nude mice. NIH3T3 cells overexpressing catalytic mutant (NIH3T3-USP2a-mut) and wild-type (NIH3T3-USP2a-wt) USP2a or infected with the empty retroviral vector (NIH3T3-EV; qPCR in *A*) were injected s.c. in nude mice. Wild-type USP2a was able to induce 0.2 to 0.9 cm^3 tumors (*B* and *C*) within 3 weeks in 12 of 12 mice injected, whereas none of the controls grew. *D,* histopathologically, these s.c. tumors show a sarcomatous phenotype (H&E in *D, ii*) and are highly proliferative as shown by BrdUrd incorporation (*D, iv*). *D, i* and *iii,* NIH3T3-EV cells by H&E and BrdUrd immunohistochemistry (*bars,* 100 μm; *inset, bars,* 50 μm).

Discussion

The USP family consists of >50 members known to date (25). Although these proteases show sequence and structural similarities at the catalytic domain site, notable divergences are present in both NH_2- and COOH-terminal ends of the proteins. In at least some cases, sequences and motifs outside the conserved catalytic domain may contribute to substrate (ubiquitin chain) and target-specificity of these isopeptidases. Importantly, whereas some USPs are known to play key regulatory roles in a variety of biological and pathologic processes, such as cellular growth pathways, stabilization/degradation of p53 protein (5, 6, 26), and DNA repair (27), only rarely do they display oncogenic properties per se (28–31). In this report, we show that USP2a is oncogenic as determined by both overexpression in nontransformed cells and knock-down in tumor cell lines.

Importantly, we report that almost half of the prostate tumors overexpress USP2a when compared with adjacent normal tissue and that these tumors display a characteristic gene expression signature. Indeed, a GSE analysis done on microarray data comparing the high and low USP2a-expressing tumors revealed that high-USP2a tumors are strongly associated with gene sets involved in both synthesis and metabolism of fatty acids, whereas only the "cell death" gene pathway, among 440 gene sets that were tested, was significantly linked with those cancers expressing low USP2a levels. Although we previously described that FAS is a substrate of USP2a (9), Stevenson et al. have shown that USP2a binds to and deubiquitinates the ubiquitin ligase Mdm2, resulting in enhanced p53 degradation.[8] The results of the gene expression profiling thus independently validate the biochemical data generated *in vitro*. To further substantiate these findings, we customized a gene set of 24 predominantly proapoptotic p53 target genes, including *apaf-1, BID, BAX, caspases 1, 6*, and *9*, as well as *p21* (32) and tested this gene set by GSEA on the same gene profiling data. As expected, this p53-related gene set was highly significantly associated with low-USP2a prostate tumors.

In USP2a-overexpressing carcinomas, genes that have been described as targets of p53-mediated suppression, were also up-regulated. In fact, we found that the gene family associated with *eea1*, recently proposed as a new p53-suppressed gene (32), was correlated with high USP2a-expressing tumors. *eea1* codifies a protein involved in important endocytic membrane fusion cell processes, such as that involved in the recycling of ErbB1 and the nuclear translocation of ErbB2 (33). Interestingly, other gene sets related to RTK family members and those controlling endocytic trafficking, such as *ErbB3* and *rab* (reviewed in refs. 34, 35), were overexpressed in tumors with high USP2a levels. ErbB2, which dimerizes with ErbB3, is overexpressed in hormone-refractory prostate cancer in the absence of genomic amplification (22, 36, 37). Furthermore, it has been suggested that cells can regulate growth factor receptor expression via ubiquitin-mediated receptor degradation. It is tempting to suggest that disruption of the degradation process by deubiquitination may result in increased expression of as yet undefined RTKs, independent of protein synthesis as a result of RTK recycling to the cell membrane for further activation (38).

Downloaded from cancerres.aacrjournals.org on May 28, 2017. © 2006 American Association for Cancer Research.

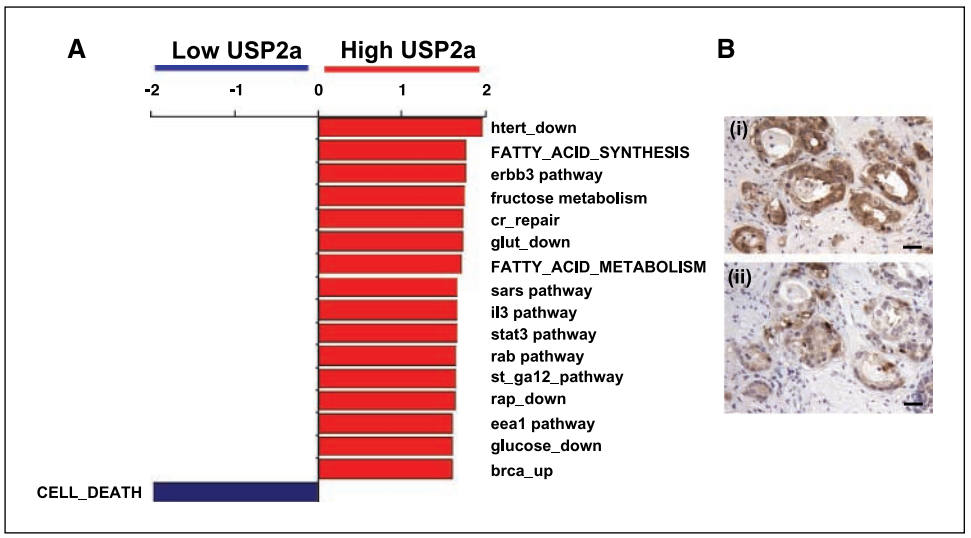

Figure 4. USP2a signature in human prostate tumors. *A,* GSEA done on gene expression profiling from the same human prostate tumors described in Fig. 1*A*. Low USP2a expressing tumors show an enrichment in cell death–related genes, whereas gene sets implicated in fatty acid synthesis and metabolism, among others, increase with USP2a levels. A complete list of gene sets is in Supplemental Table S1 (http://www.broad.mit.edu/cgi-bin/cancer/datasets.cgi). *B,* representative example of immunohistochemistry for FAS (*i*) and Mdm2 (*ii*) done on a case of paraffin-embedded prostate tumor overexpressing USP2a (*bars,* 100 μm).

USP2a silencing caused significant apoptosis in most of the cell lines tested. Destabilization of both FAS and Mdm2 could be invoked as causes of programmed cell death but the relative role played by each of these pathways, when disrupted, is currently not known and may vary in different cell lines according to FAS expression levels and p53 status. FAS has been shown to play a significant role in protecting tumor cells from apoptosis. In fact, FAS inhibitors as well as RNA interference of FAS message, result in apoptosis of cancer cells (39) and decrease the size of prostate cancer xenografts that overexpress the enzyme (40). We had previously shown that apoptosis induced by USP2a interference could be rescued by FAS overexpression (9). The mechanisms invoked include the accumulation of malonyl-CoA (41, 42) and the inhibition of fatty acid β-oxidation (43). More importantly, FAS has been hypothesized to restore mitochondrial membrane potential, preventing the initiation of the apoptotic cascade. It has been shown that FAS inhibition results in the release of cytochrome *c*. In fact, apoptosis induced by the FAS inhibitor cerulenin is characterized by the rapid mitochondrial release of cytochrome *c* both in wild-type and mutant p53 cell lines (44). The precise mechanisms by which FAS inhibition leads to apoptosis, however, are still unclear.

The proapoptotic activity occurring when USP2a is silenced can also be ascribed to p53 up-regulation resulting from Mdm2 destabilization[8] (Fig. 5*C*). Interestingly, LNCaP cells might represent a good example of the dual USP2a-mediated antiapoptotic mechanism, via both FAS and Mdm2, because these cells express both high levels of FAS and functional p53. In support of this contention, when compared with p53-negative cell lines, LNCaP cells show the highest levels of apoptosis following exposure to USP2a siRNA.

Taken together, these findings suggest that USP2a is involved in human tumorigenesis by participating directly and indirectly with different crucial pathways affecting the apoptotic machinery. We provided evidence that ectopic USP2a expression in immortalized prostate epithelial cells rendered them resistant to both taxol and cisplatin-induced apoptosis, suggesting that increasing USP2a levels allow tumor cells to escape chemotherapy-induced programmed cell death. The emerging role of taxane-based drug treatments in the clinical management of prostate cancer (13, 45) highlights the importance of being able to define subsets of patients potentially refractory to this therapy. To this end, the immediate implications of our results are that human tumors overexpressing USP2a can be identified as resistant to commonly used chemotherapeutic agents.

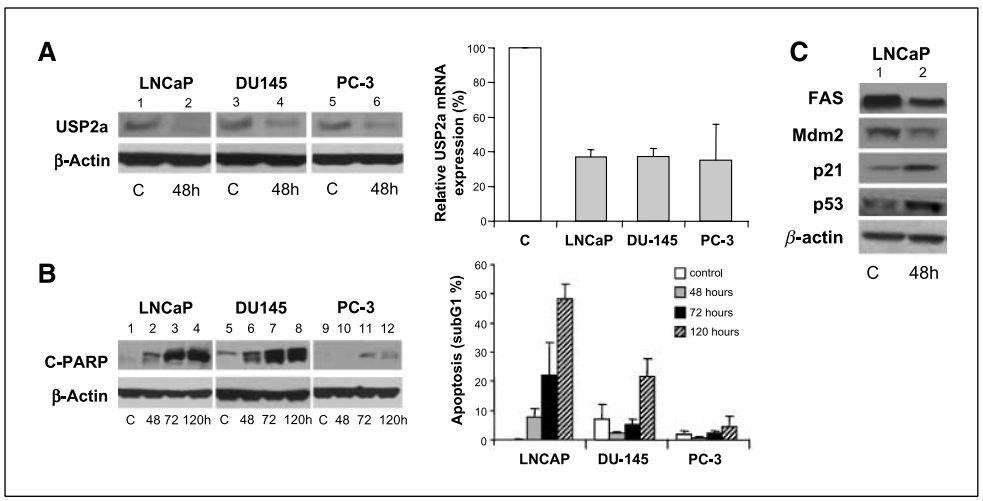

Figure 5. USP2a protects prostate cancer cells from apoptosis. USP2a-siRNA was transfected into LNCaP, DU145, and PC-3 cells. *A,* USP2a knockdown, shown by Western blot (*left, lanes 2, 4*, and *6 top row*) and qRT-PCR (*right*) induced apoptosis in LNCaP and DU145 cells, and minimally in PC-3 cells as well. *B,* apoptosis was assayed by Western blot for cleaved-PARP (*left*) and propidium iodide staining with FACS analysis (*right*). USP2a-siRNA was transfected in LNCaP cells and cell lysates were examined for FAS, Mdm2, p21, and p53 at 48 hours (*C*).

Downloaded from cancerres.aacrjournals.org on May 28, 2017. © 2006 American Association for Cancer Research.

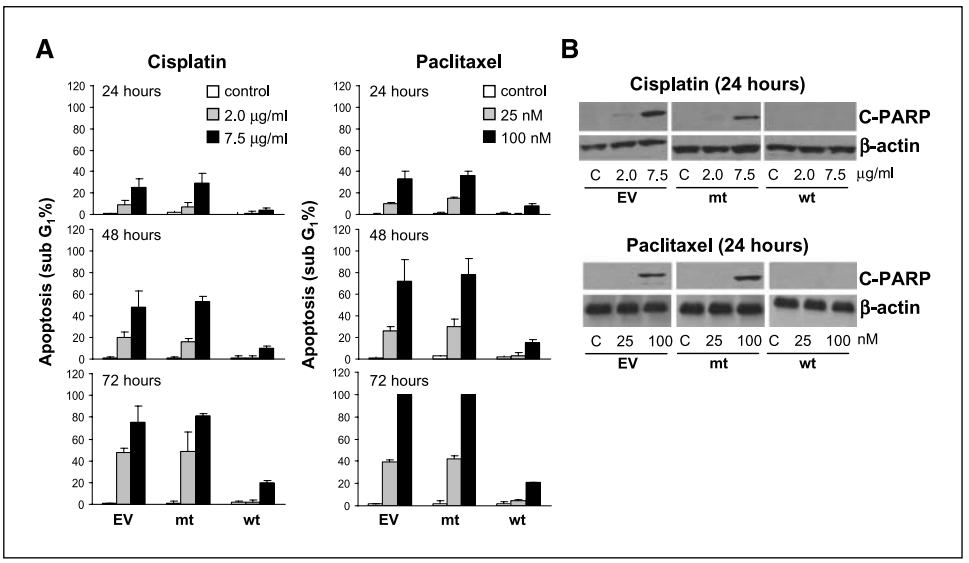

Figure 6. USP2a confers resistance to apoptosis to immortalized nontransformed prostate epithelial cells. Protection from apoptosis induced by chemotherapeutic agents (*A* and *B*). Apoptosis assays were done as described in Fig. 5*B* in AR-iPrEC-pBABE (*EV*), AR-iPREC-USP2a-mut (*mut*), and AR-iPREC-USP2a-wt (*wt*) cells following 24, 48, and 72 hours of treatment with cisplatin [doses 2.0 (*gray columns*) and 7.5 μg/mL (*black columns*)] and paclitaxel [doses 25 (*gray columns*) and 100 nmol/L (*black columns*)].

Therefore, the data we provided suggest that USP2a represents a therapeutic target in human cancer. Importantly, the crystal structures of both USP2[9] and FAS (14) have been solved, and this will undoubtedly boost the drug discovery efforts of small molecule inhibitors of both these molecules.

In summary, we show that USP2a is oncogenic when overexpressed both *in vitro* and *in vivo* and this oncogenic potential is related to its antiapoptotic activity. Gene expression profiling of human prostate tumors confirmed that the antiapoptotic role of USP2a is mediated by its enzymatic activity on both FAS and Mdm2. Taken together, these results provide the biological rationale for USP2a targeting in human cancer.

Acknowledgments

Received 4/13/2006; revised 5/26/2006; accepted 6/28/2006.

Grant support: NIH (Specialized Programs of Research Excellence 5P50CA90381, PO1 CA089021), and the Prostate Cancer Foundation (M. Loda). M. Loda is a consultant for Novartis Pharmaceuticals, Inc., and is a member of the Center for Cancer Genome Discovery, Dana Farber Cancer Institute. P.G. Febbo is a Damon Runyon Cancer Research Clinical Investigator and receives additional support from the Prostate Cancer Foundation. A. Farsetti receives funds from Associazione Italiana Ricerca sul Cancro and Ministero della Salute, Italy. A. Porrello is supported by a grant from Alleanza Contro il Cancro-Genomica 2004, Ministero della Salute, Italy.

The costs of publication of this article were defrayed in part by the payment of page charges. This article must therefore be hereby marked *advertisement* in accordance with 18 U.S.C. Section 1734 solely to indicate this fact.

We thank Dr. William C. Hahn for kindly providing immortalized prostate epithelial cells and Drs. Saville (University of Dundee, Dundee, Scotland) and Renatus (Novartis Pharmaceuticals, Basel, Switzerland) for sharing their data prior to publication.

References

1. Amerik AY, Hochstrasser M. Mechanism and function of deubiquitinating enzymes. Biochim Biophys Acta 2004;1695:189–207.
2. Goldberg AL. Functions of the proteasome: the lysis at the end of the tunnel. Science 1995;268:522–3.
3. Wilkinson KD. Ubiquitination and deubiquitination: targeting of proteins for degradation by the proteasome. Semin Cell Dev Biol 2000;11:141–8.
4. Cummins JM, Rago C, Kohli M, Kinzler KW, Lengauer C, Vogelstein B. Tumour suppression: disruption of HAUSP gene stabilizes p53. Nature 2004;428:1 p following 486.
5. Cummins JM, Vogelstein B. HAUSP is required for p53 destabilization. Cell Cycle 2004;3:689–92.
6. Li M, Brooks CL, Kon N, Gu W. A dynamic role of HAUSP in the p53-2 pathway. Mol Cell 2004;13:879–86.
7. Brummelkamp TR, Nijman SM, Dirac AM, Bernards R. Loss of the cylindromatosis tumour suppressor inhibits apoptosis by activating NF-κB. Nature 2003;424:797–801.
8. Kovalenko A, Chable-Bessia C, Cantarella G, Israel A, Wallach D, Courtois G. The tumour suppressor CYLD negatively regulates NF-κB signalling by deubiquitination. Nature 2003;424:801–5.
9. Graner E, Tang D, Rossi S, et al. The isopeptidase USP2a regulates the stability of fatty acid synthase in prostate cancer. Cancer Cell 2004;5:253–61.
10. Baron A, Migita T, Tang D, Loda M. Fatty acid synthase: a metabolic oncogene in prostate cancer? J Cell Biochem 2004;91:47–53.
11. Stewart AB, Lwaleed BA, Douglas DA, Birch BR. Current drug therapy for prostate cancer: an overview. Curr Med Chem Anti-Canc Agents 2005;5:603–12.
12. Armstrong AJ, Carducci MA. Novel therapeutic approaches to advanced prostate cancer. Clin Adv Hematol Oncol 2005;3:271–82.
13. Febbo PG, Richie JP, George DJ, et al. Neoadjuvant docetaxel before radical prostatectomy in patients with high-risk localized prostate cancer. Clin Cancer Res 2005;11:5233–40.
14. Maier T, Jenni S, Ban N. Architecture of mammalian fatty acid synthase at 4.5 Å resolution. Science 2006;311:1258–62.
15. Berger R, Febbo PG, Majumder PK, et al. Androgen-induced differentiation and tumorigenicity of human prostate epithelial cells. Cancer Res 2004;64:8867–75.
16. Schiffer IB, Gebhard S, Heimerdinger CK, et al. Switching off HER-2/neu in a tetracycline-controlled mouse tumor model leads to apoptosis and tumor-size-dependent remission. Cancer Res 2003;63:7221–31.
17. Singh D, Febbo PG, Ross K, et al. Gene expression correlates of clinical prostate cancer behavior. Cancer Cell 2002;1:203–9.
18. Livak KJ, Schmittgen TD. Analysis of relative gene expression data using real-time quantitative PCR and the 2(−ΔΔC(T)) method. Methods 2001;25:402–8.
19. Subramanian A, Tamayo P, Mootha VK, et al. Gene set enrichment analysis: a knowledge-based approach for interpreting genome-wide expression profiles. Proc Natl Acad Sci U S A 2005;102:15545–50.
20. Rossi S, Graner E, Febbo P, et al. Fatty acid synthase expression defines distinct molecular signatures in prostate cancer. Mol Cancer Res 2003;1:707–15.
21. Gousseva N, Baker RT. Gene structure, alternate splicing, tissue distribution, cellular localization, and developmental expression pattern of mouse deubiquitinating enzyme isoforms Usp2-45 and Usp2-69. Gene Expr 2003;11:163–79.
22. Signoretti S, Montironi R, Manola J, et al. Her-2-neu expression and progression toward androgen independence in human prostate cancer. J Natl Cancer Inst 2000;92:1918–25.
23. Li Z, Szabolcs M, Terwilliger JD, Efstratiadis A. Prostatic intraepithelial neoplasia and adenocarcinoma in mice expressing a probasin-Neu oncogenic transgene. Carcinogenesis 2006;27:1054–67.
24. Alvarez JV, Febbo PG, Ramaswamy S, Loda M, Richardson A, Frank DA. Identification of a genetic signature of activated signal transducer and activator of transcription 3 in human tumors. Cancer Res 2005;65:5054–62.
25. Nijman SM, Luna-Vargas MP, Velds A, et al. A genomic and functional inventory of deubiquitinating enzymes. Cell 2005;123:773–86.
26. Li M, Chen D, Shiloh A, et al. Deubiquitination of p53 by HAUSP is an important pathway for p53 stabilization. Nature 2002;416:648–53.
27. Huang TT, Nijman SM, Mirchandani KD, et al. Regulation of monoubiquitinated PCNA by DUB autocleavage. Nat Cell Biol 2006;8:339–47.
28. Gupta K, Copeland NG, Gilbert DJ, Jenkins NA, Gray DA. Unp, a mouse gene related to the tre oncogene. Oncogene 1993;8:2307–10.

Downloaded from cancerres.aacrjournals.org on May 28, 2017. © 2006 American Association for Cancer Research.

29. Frederick A, Rolfe M, Chiu MI. The human UNP locus at 3p21.31 encodes two tissue-selective, cytoplasmic isoforms with deubiquitinating activity that have reduced expression in small cell lung carcinoma cell lines. Oncogene 1998;16:153–65.
30. Gupta K, Chevrette M, Gray DA. The Unp proto-oncogene encodes a nuclear protein. Oncogene 1994;9: 1729–31.
31. DeSalle LM, Latres E, Lin D, et al. The de-ubiquitinating enzyme Unp interacts with the retino-blastoma protein. Oncogene 2001;20:5538–42.
32. Wei CL, Wu Q, Vega VB, et al. A global map of p53 transcription-factor binding sites in the human genome. Cell 2006;124:207–19.
33. Giri DK, Ali-Seyed M, Li LY, et al. Endosomal transport of ErbB-2: mechanism for nuclear entry of the cell surface receptor. Mol Cell Biol 2005;25:11005–18.
34. Szymkiewicz I, Shupliakov O, Dikic I. Cargo- and compartment-selective endocytic scaffold proteins. Bio-chem J 2004;383:1–11.
35. Hoekstra D, Tyteca D, van IJzendoorn SC. The subapical compartment: a traffic center in membrane polarity development. J Cell Sci 2004;117:2183–92.
36. Bartlett JM, Brawley D, Grigor K, Munro AF, Dunne B, Edwards J. Type I receptor tyrosine kinases are associated with hormone escape in prostate cancer. J Pathol 2005;205:522–9.
37. Hernes E, Fossa SD, Berner A, Otnes B, Nesland JM. Expression of the epidermal growth factor receptor family in prostate carcinoma before and during androgen-independence. Br J Cancer 2004;90:449–54.
38. Sweeney C, Carraway KL. 3rd Negative regulation of ErbB family receptor tyrosine kinases. Br J Cancer 2004; 90:289–93.
39. Kuhajda FP. Fatty-acid synthase and human cancer: new perspectives on its role in tumor biology. Nutrition 2000;16:202–8.
40. Pizer ES, Pflug BR, Bova GS, Han WF, Udan MS, Nelson JB. Increased fatty acid synthase as a therapeutic target in androgen-independent prostate cancer pro-gression. Prostate 2001;47:102–10.
41. Pizer ES, Thupari J, Han WF, et al. Malonyl-coenzyme-A is a potential mediator of cytotoxicity induced by fatty-acid synthase inhibition in human breast cancer cells and xenografts. Cancer Res 2000;60: 213–8.
42. De Schrijver E, Brusselmans K, Heyns W, Verhoeven G, Swinnen JV. RNA interference-mediated silencing of the fatty acid synthase gene attenuates growth and induces morphological changes and apoptosis of LNCaP prostate cancer cells. Cancer Res 2003;63:3799–804.
43. Thupari JN, Pinn ML, Kuhajda FP. Fatty acid synthase inhibition in human breast cancer cells leads to malonyl-CoA-induced inhibition of fatty acid oxidation and cytotoxicity. Biochem Biophys Res Commun 2001; 285:217–23.
44. Heiligtag SJ, Bredehorst R, David KA. Key role of mitochondria in cerulenin-mediated apoptosis. Cell Death Differ 2002;9:1017–25.
45. Cabrespine A, Guy L, Khenifar E, et al. Randomized phase II study comparing paclitaxel and carboplatin versus mitoxantrone in patients with hormone-refractory prostate cancer. Urology 2006;67:354–9.

Downloaded from cancerres.aacrjournals.org on May 28, 2017. © 2006 American Association for Cancer Research.

AACR American Association for Cancer Research

Cancer Research
The Journal of Cancer Research (1916–1930) | The American Journal of Cancer (1931–1940)

The Isopeptidase USP2a Protects Human Prostate Cancer from Apoptosis

Carmen Priolo, Dan Tang, Mohan Brahamandan, et al.

Cancer Res 2006;66:8625-8632.

Updated version	Access the most recent version of this article at: http://cancerres.aacrjournals.org/content/66/17/8625
Supplementary Material	Access the most recent supplemental material at: http://cancerres.aacrjournals.org/content/suppl/2006/09/08/66.17.8625.DC1

Cited articles	This article cites 44 articles, 14 of which you can access for free at: http://cancerres.aacrjournals.org/content/66/17/8625.full.html#ref-list-1
Citing articles	This article has been cited by 23 HighWire-hosted articles. Access the articles at: /content/66/17/8625.full.html#related-urls

E-mail alerts	Sign up to receive free email-alerts related to this article or journal.
Reprints and Subscriptions	To order reprints of this article or to subscribe to the journal, contact the AACR Publications Department at pubs@aacr.org.
Permissions	To request permission to re-use all or part of this article, contact the AACR Publications Department at permissions@aacr.org.

Downloaded from cancerres.aacrjournals.org on May 28, 2017. © 2006 American Association for Cancer Research.